Title

On the effect and robustness of zero-crossing detection algorithms in simulation of hybrid systems jumping on surfaces

ISBN

9781457710957

Authors

Copp, DA
Sanfelice, RG

Publication Date

2012

DOI

10.1109/acc.2012.6315684

Peer reviewed

On the Effect and Robustness of Zero-crossing Detection Algorithms in Simulation of Hybrid Systems Jumping on Surfaces

David A. Copp and Ricardo G. Sanfelice

***Abstract*— Motivated by the fragility to perturbations of hybrid systems jumping on surfaces and the robustifying capabilities of zero-crossing detection algorithms, we propose a hybrid simulator model with incorporated zero-crossing detection. First, we reveal the effect of measurement noise and of discretization to hybrid systems jumping on surfaces. We prove that, under mild regularity conditions, zero-crossing detection algorithms have a robustifying effect on the original system. Then, we argue that, rather than computing the solutions to the discretization of the fragile nominal model, integration schemes with zero-crossing detection actually compute the solutions of a robustified version of the original model. We propose a mathematical model for the hybrid system with incorporated zero-crossing detection as well as a hybrid simulator for it. We show that both the model and simulator are not only robust, but also that the hybrid simulator preserves asymptotic stability properties, semiglobally and practically (on the step size), of the original system. An example illustrates the ideas and results throughout the paper.**

I. Introduction

We consider dynamical systems with a state that experiences instantaneous resets (jumps) when it hits a *switching surface* $\mathcal{S}$. Switching surfaces are typically defined as the zero-level set of a continuously differentiable function, defining in this way a codimension one submanifold of $\mathbb{R}^n$; see, e.g., [1], [2], [3]. Denoting the state by x, which takes values from a region of operation $\mathcal{X} \subset \mathbb{R}^n$, the continuous dynamics of the system are given by a differential equation when x is away from the surface. More precisely, the flows are governed by

$$\dot{x} = f(x) \qquad \text{when } x \in \mathcal{X} \setminus \mathcal{S}. \tag{1}$$

When x hits the surface while in the region of operation, the state is reset via a difference equation defining the jumps of the system. More precisely, the new value of x after the jump, denoted x^+, is determined via

$$x^+ = g(x) \qquad \text{when } x \in \mathcal{S} \cap \mathcal{X}. \tag{2}$$

In this way, the trajectories are allowed to flow when $x \in \mathcal{X} \setminus \mathcal{S}$ and are allowed to jump when $x \in \mathcal{S} \cap \mathcal{X}$. This model captures the dynamics of control systems in which a controller makes decisions when certain variables belong to a surface. For instance, in reset control systems (see, e.g., [4], [5], [6], [7]), the output of the controller is reset to zero whenever its input and output satisfy an algebraic condition. In state-dependent impulsive control systems, (see, e.g., [8], [9]), jumps occur when the state of the systems belongs to a surface in the state space of the system.

There are several difficulties associated with systems jumping on surfaces. For instance, suppose that the value of the state x of the system is perturbed when nearby $\mathcal{S}$ (e.g., due to measurement noise). Let e denote this perturbation. Suppose that, for a given solution $x(t)$ to system (1)-(2) (using an appropriate notion of solution), e is zero when $x(t) \neq \mathcal{S}$ but equal to a nonzero constant ε when $x(t) = \mathcal{S}$. Then, when the perturbation e is added, for any nonzero ε, the same solution $x(t)$ will not satisfy the condition $x(t) + e(t) \in \mathcal{S}$ as before, and therefore, will not jump at the instant it was jumping without noise. This suggests that arbitrarily small perturbations to (1)-(2) can generate trajectories that are nowhere close to the trajectories of the nominal system; see [10] for related discussions. The same issue appears in numerical simulations of such a system because integration errors introduced by the discretization prevents the computed solution from belonging to the switching surface. To remedy this problem, algorithms to detect "crossings" of the switching surface are typically employed.

In this paper, we propose a mathematical model for hybrid systems with zero-crossing detection as well as a hybrid simulator for it. As a difference to [11], [12], we focus on detection of zero-crossing rather than accurate location. After revealing the effect of measurement noise and of discretization to hybrid systems jumping on surfaces, we show that both the model and simulator are not only robust, but also that the simulator preserves asymptotic stability properties, semiglobally and practically (on the step size), of the original system. The results are illustrated in an example throughout the paper.

The remainder of this paper is organized as follows. Section II presents a mathematical model of hybrid systems with dynamics (1)-(2), a hybrid simulator for it, and issues with perturbations. A model of a hybrid system with added zero-crossing detection and associated hybrid simulator are in Section III. Our main results appear in Section IV.

II. Hybrid Systems Jumping on Surfaces

In this paper, we model systems and their simulators within the hybrid systems framework of [13] and [14]. In this way, we write system (1)-(2) as

$$\mathcal{H}: \quad \begin{cases} \dot{x} &= f(x) & x \in \mathcal{X} \setminus \mathcal{S} =: C \\ x^+ &= g(x) & x \in \mathcal{S} \cap \mathcal{X} =: D. \end{cases} \tag{3}$$

D. A. Copp and R. G. Sanfelice are with the Department of Aerospace and Mechanical Engineering, University of Arizona, 1130 N. Mountain Ave, AZ 85721, USA. Email: dacopp,sricardo@u.arizona.edu
Research partially supported by the National Science Foundation under CAREER Grant no. ECS-1150306.

Following [13], a solution to a hybrid system is a function defined on a hybrid time domain satisfying certain conditions. A set $E \subset \mathbb{R}_{\geq 0} \times \mathbb{N}$ is a *compact hybrid time domain* if

$$E = \bigcup_{j=0}^{J-1} ([t_j, t_{j+1}] \times \{j\})$$

for some finite sequence of times $0 = t_0 \leq t_1 \leq t_2 ... \leq t_J$. The set E is a *hybrid time domain* if for all $(T, J) \in E$, $E \cap ([0, T] \times 0, 1, ...J)$ is a compact hybrid domain. By *hybrid arc* or *hybrid trajectory* we understand a pair consisting of a hybrid time domain $\operatorname{dom} x$ and a function $x : \operatorname{dom} x \to \mathbb{R}^n$ such that, for each j, $t \mapsto x(t, j)$ is locally absolutely continuous for $(t, j) \in \operatorname{dom} x$. A hybrid arc $\phi : \operatorname{dom} \phi \to \mathbb{R}^n$ is a *solution* to a hybrid system $\mathcal{H}$ with data (C, f, D, g) if

(S0) $\phi(0, 0) \in C \cup D$;

(S1) For each $j \in \mathbb{N}$ and each $I_j := \{t : (t, j) \in \operatorname{dom} \phi\}$ with nonempty interior int I_j,

$$\begin{array}{ll} \phi(t, j) \in C & \text{for all } t \in \text{int } I_j \\ \dot{\phi}(t, j) = f(\phi(t, j)) & \text{for almost all } t \in \text{int } I_j; \end{array} \quad (4)$$

(S2) For each $(t, j) \in \operatorname{dom} \phi$ such that $(t, j + 1) \in \operatorname{dom} \phi$,

$$\phi(t, j) \in D, \quad \phi(t, j + 1) = g(\phi(t, j)). \quad (5)$$

Now, we consider an example of a hybrid system model that includes switching surfaces.

Example 2.1: (unicycle avoiding obstacle) Consider a mobile robot of the unicycle type being steered towards a target while avoiding a circular obstacle [2]. Let $x = [\xi^\top, q]^\top$, where $\xi = [\xi_1, \xi_2]^\top$ is the vehicle position, $(\xi_1^\circ, \xi_2^\circ)$ is the obstacle position, and q is the controller state, $q \in \{1, 2\}$, where $q = 1$ means go towards the target, and $q = 2$ means go away from obstacle. The modes are chosen depending on the robot's radial distance from the obstacle. Two circular surfaces $\mathcal{S}_q$ with radii $a_q, a_2 > a_1$, are defined around the obstacle for this purpose.

The closed-loop system is given by

$$\mathcal{X} = \mathbb{R}^2 \times \{1, 2\}, \quad (6)$$

$$f(x) = \begin{bmatrix} v \cos(\kappa(q, \xi)) \\ v \sin(\kappa(q, \xi)) \\ 0 \end{bmatrix}, \quad g(x) = \begin{bmatrix} \xi \\ 3 - q \end{bmatrix} \quad (7)$$

$$\mathcal{S} = \cup_{q \in \{1,2\}} (\mathcal{S}_q \times \{q\}) \quad (8)$$

$$\mathcal{S}_q = \left\{ \xi \in \mathbb{R}^2 : (\xi_1^\circ - \xi_1)^2 + (\xi_2^\circ - \xi_2)^2 = a_q^2 \right\}, \quad (9)$$

where v is the tangential velocity of the robot, and the function $\kappa(q, \xi)$ defines the mode-based controller which the robot should use in order to steer the robot to the target or away from the obstacle.

As pointed out in Section I, arbitrarily small measurement noise can prevent the robot from switching modes when reaching a boundary. This could lead the robot to collide with the obstacle or move away from the target. Next we will discuss these nonrobust properties. $\triangle$

A. Nonrobustness to measurement noise

As pointed out in Section I, when noise is present in the measurements of the state x, solutions to $\mathcal{H}$ may fail to jump due to never belonging to the surface. In fact, for every nominal solution to $\mathcal{H}$, it is possible to construct an arbitrarily small measurement noise signal e so that $x + e \in \mathcal{S}$ never holds. A hybrid system $\mathcal{H}$ with data (C, f, D, g) and measurement noise $e : \operatorname{dom} e \to \mathbb{R}^n$ is denoted $\mathcal{H}^e$ and is given by

$$\mathcal{H}^e : \quad \begin{cases} \dot{x} = f(x + e) & x + e \in C \\ x^+ = g(x + e) & x + e \in D. \end{cases} \quad (10)$$

A *solution* to $\mathcal{H}$ with measurement noise e, that is, a solution to $\mathcal{H}^e$ for a given measurement noise e, consists of a hybrid arc $\phi^e : \operatorname{dom} \phi^e \to \mathbb{R}^n$ satisfying

(S0^e) $\phi^e(0, 0) + e(0, 0) \in C \cup D$;

(S1^e) For each $j \in \mathbb{N}$ and each $I_j = \{t : (t, j) \in \operatorname{dom} \phi^e\}$ with nonempty interior int I_j,

$$\begin{array}{ll} \phi^e(t, j) + e(t, j) \in C & \text{for all } t \in \text{int } I_j \\ \dot{\phi}^e(t, j) = f(\phi^e(t, j) + e(t, j)) & \text{for almost all } t \in \text{int } I_j; \end{array}$$

(S2^e) For each $(t, j) \in \operatorname{dom} \phi^e$ such that $(t, j + 1) \in \operatorname{dom} \phi^e$,

$$\phi^e(t, j) + e(t, j) \in D, \quad \phi^e(t, j + 1) = g(\phi^e(t, j) + e(t, j)).$$

The following result formalizes the fact that arbitrarily small measurement noise may prevent solutions to $\mathcal{H}$ from jumping on $\mathcal{S}$. Below, we say that a function $\ell : \mathbb{R}^n \to \mathbb{R}^n$ is locally bounded on an open set O if for each compact set $K \subset O$ there exists a compact set $K' \subset \mathbb{R}^n$ such that $\ell(K) \subset K'$.

Proposition 2.2: (no jumps due to measurement noise) Suppose $\mathcal{H} = (C, f, D, g)$ as in (3) *is such that*

1) *$f : \mathbb{R}^n \to \mathbb{R}^n$ and $g : \mathbb{R}^n \to \mathbb{R}^n$ are locally bounded on an open set containing $\mathcal{X}$;*
2) *$\mathcal{S} \cap \mathcal{X}$ is a codimension one submanifold of $\mathbb{R}^n$.*

Then, for each $\varepsilon > 0$, each $T > 0$, and each $x_0 \in \mathcal{X}$, every solution ϕ^e to $\mathcal{H}$ with measurement noise e and $\phi^e(0, 0) = x_0$ satisfies $\operatorname{dom} \phi^e \subset [0, T] \times \{0\}$, for some (solution dependent) measurable function $e : \operatorname{dom} e \to \varepsilon \mathbb{B}$.

B. Properties of numerical simulations of $\mathcal{H}$

The simulation of $\mathcal{H}$ can be interpreted as the numerical computation of the solutions to the discretized version of $\mathcal{H}$, defining a simulator. A *hybrid simulator for $\mathcal{H}$* will be given by the family of systems $\mathcal{H}^s$ parameterized by step size s satisfying $s \in (0, s^*]$, with $s^* > 0$ being the maximum step size. The data of the hybrid simulator $\mathcal{H}^s$ is denoted by (C^s, f^s, D^s, g^s). For simplicity, we will assume that the region of operation $\mathcal{X}$ is not discretized. Following [14], a hybrid simulator $\mathcal{H}^s$ for the hybrid system $\mathcal{H}$ is written as

$$\mathcal{H}^s \begin{cases} x_s^+ = f^s(x_s) & x_s \in \mathcal{X} \setminus \mathcal{S}^s =: C^s \\ x_s^+ = g^s(x_s) & x_s \in \mathcal{S}^s \cap \mathcal{X} =: D^s. \end{cases} \quad (11)$$

Comparing $\mathcal{H}$ with $\mathcal{H}^s$, the dynamics for the flows of $\mathcal{H}$ have been replaced by the integration scheme $x_s^+ = f^s(x_s)$,

where f^s is constructed from f. The jump map of $\mathcal{H}$ has been replaced by the discretized map g^s while the flow and jump sets C and D have been replaced by the discretized sets C^s and D^s, where $\mathcal{S}^s$ is the discretization of $\mathcal{S}$. Being that the dynamics of the hybrid simulator $\mathcal{H}^s$ are purely discrete, the solutions to $\mathcal{H}^s$ are given on discrete versions of hybrid time domains. Instead of (t, j), we use (k, j) to parametrize solutions to $\mathcal{H}^s$. (See [14] for more details.)

A similar behavior to that in Proposition 2.2 highlighting lack of robustness to measurement noise arises in numerical simulations of hybrid systems, where the numerical approximations play the role of measurement noise. For example, when implementing the hybrid system $\mathcal{H}$ in a simulator, the discretization in time produced by the ODE solver may prevent jumps from being triggered since the condition $x_s \in \mathcal{S}^s$ may never hold. To illustrate this, consider the case of the flow map f being discretized with an Euler integration scheme. It follows that for every $s^* > 0$ and each $x_0 \in \mathcal{X}$, every solution ϕ^s to $\mathcal{H}^s$ with some step size $s \in (0, s^*]$ and $\phi^s(0,0) = x_0$ satisfies $\operatorname{dom} \phi^s \subset \mathbb{N} \times \{0\}$, where s is a (solution dependent) step size. In fact, fix the initial condition $x_0 \in \mathcal{X}$. Suppose that for each $s \in (0, s^*]$ and every solution ϕ^s to $\mathcal{H}_s$, we have $\phi^s(k^*, 0) \in \mathcal{S}^s$ for some $k^* \in \mathbb{N}$ (depending on s and ϕ^s). Then, by definition of solution to $\mathcal{H}^s$, we have $\phi^s(k, 0) = f^s(\phi^s(k-1, 0))$ for each $k = 1, 2, \ldots, k^*$ with $\phi^s(0,0) = x_0$. Equivalently, we can write that $\phi^s(k^*, 0) = f^s \circ f^s \circ \ldots \circ f^s(x_0) =: (f^s)^{k^*}(x_0)$, where $(f^s)^{k^*}$ denotes k^* compositions of f^s. By continuity in s of the resulting map, we have that $\phi^s(k^*, 0)$ cannot be in $\mathcal{S}^s$ for each s.

Now, we illustrate this issue by revisiting Example 2.1.

Example 2.3: (unicycle avoiding obstacle (revisited)) For the hybrid system in Example 2.1, consider a hybrid simulator $\mathcal{H}^s$ with $g^s = g$, $\mathcal{S}^s = \mathcal{S}$, and f^s given by the Euler integration scheme, i.e., $f^s(x) = x + sf(x) = x + s\left[v\cos(\kappa(q,\xi)), v\sin(\kappa(q,\xi)), 0\right]^\top$. The robot changes steering modes when it crosses the surface $\mathcal{S}_q$ in order to steer the robot away from the obstacle and towards the target. Figure 1 shows a solution of a robot using the controller in [2] starting at $(\xi_1, \xi_2) = (0, 0)$ moving towards the green target while operating in mode $q = 1$. The obstacle is at $(\xi_1^\circ, \xi_2^\circ) = (35, 35)$ with radius smaller than a_1, while $a_1 = 15$ and $a_2 = 20$. Figure 1(a) shows a solution where the robot enters surface $\mathcal{S}_2$, changes mode to $q = 2$ to move away from the obstacle, and then, due to discretization effects, steps over $\mathcal{S}_1$ and fails to change mode back to $q = 1$. Figure 1(b) represents the opposite situation, where a jump to mode $q = 2$ is not triggered and a collision with the obstacle could take place. Both of these cases can occur due to numerical error in the simulation. △

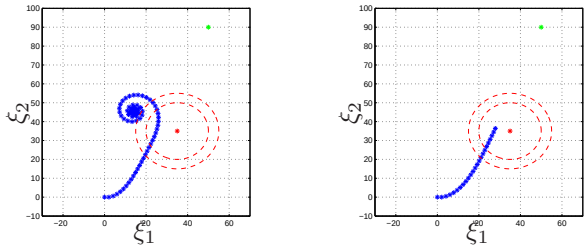

(a) Solution of robot missing mode change and never reaching target.

(b) Solution of robot missing mode change.

Fig. 1. Solutions to the unicycle system in Example 2.1 that do not capture mode changes. The target is located at $(50, 90)$.

III. A HYBRID MODEL FOR HYBRID SYSTEMS JUMPING ON SURFACES WITH ZERO-CROSSING DETECTION

A. A hybrid system model of $\mathcal{H}$ with zero-crossing detection

For the simulation of nonlinear systems, software packages use special algorithms to capture when solutions hit a surface. In general, these algorithms involve a memory state z and a function that changes sign according to the location of x with respect to $\mathcal{S}$. We call such a function a *zero-crossing function*.

Definition 3.1 (zero-crossing function): A *zero-crossing function on a set $\mathcal{X} \subset \mathbb{R}^n$ for a switching surface $\mathcal{S}$* is given by a function $h : \mathcal{X} \to \mathbb{R}$ that implicitly characterizes $\mathcal{S}$ and splits $\mathcal{X}$ into subspaces $\mathcal{X}_1, \mathcal{X}_2 \subset \mathbb{R}^n$ as follows:

$$\mathcal{S} \cap \mathcal{X} = \{x \in \mathcal{X} : h(x) = 0\}, \quad (12)$$
$$\mathcal{X}_1 = \{x \in \mathcal{X} : h(x) < 0\}, \quad (13)$$
$$\mathcal{X}_2 = \{x \in \mathcal{X} : h(x) > 0\}, \quad (14)$$

where $\mathcal{X} = \mathcal{S} \cup \mathcal{X}_1 \cup \mathcal{X}_2$.

For Example 2.1, a zero-crossing function h on $\mathcal{X} = \mathbb{R}^2 \times \{1, 2\}$ for $\mathcal{S}$ as in (8) is given by

$$h(x) = h_q(x) := (\xi_1^\circ - \xi_1)^2 + (\xi_2^\circ - \xi_2)^2 - a_q^2$$

and the sets $\mathcal{X}_1$ and $\mathcal{X}_2$ become

$$\begin{aligned}\mathcal{X}_1 &= \left(\left\{\xi \in \mathbb{R}^2 \ : \ h_1(\xi) < 0 \right\} \times \{1\}\right) \\ &\quad \cup \left(\left\{\xi \in \mathbb{R}^2 \ : \ h_2(\xi) < 0 \right\} \times \{2\}\right), \\ \mathcal{X}_2 &= \left(\left\{\xi \in \mathbb{R}^2 \ : \ h_1(\xi) > 0 \right\} \times \{1\}\right) \\ &\quad \cup \left(\left\{\xi \in \mathbb{R}^2 \ : \ h_2(\xi) > 0 \right\} \times \{2\}\right).\end{aligned}$$

A version of the hybrid system $\mathcal{H}$ with zero-crossing detection capabilities is denoted $\mathcal{H}_{\text{ZCD}} = (C_{\text{ZCD}}, f_{\text{ZCD}}, D_{\text{ZCD}}, g_{\text{ZCD}})$ and is given by

$$\begin{aligned}\begin{bmatrix} \dot{x} \\ \dot{z} \end{bmatrix} &= \begin{bmatrix} f(x) \\ 0 \end{bmatrix} =: f_{\text{ZCD}}(x) \qquad (x, z) \in C_{\text{ZCD}} \\ \begin{bmatrix} x^+ \\ z^+ \end{bmatrix} &= \begin{bmatrix} g(x) \\ h(g(x)) \end{bmatrix} =: g_{\text{ZCD}}(x) \qquad (x, z) \in D_{\text{ZCD}},\end{aligned} \quad (15)$$

where $z \in \mathbb{R}$ is a memory state, h is a *zero-crossing function* on $\mathcal{X}$ for $\mathcal{S}$, and

$$C_{\text{ZCD}} := \{(x, z) \in \mathcal{X} \times \mathbb{R} \ : \ h(x)z \geq 0 \}, \quad (16)$$
$$D_{\text{ZCD}} := \{(x, z) \in \mathcal{X} \times \mathbb{R} \ : \ h(x)z \leq 0 \}. \quad (17)$$

The memory state z is added here to keep track of whether the state x is in the side of $\mathcal{S}$ with h negative ($x \in \mathcal{X}_1$) or in the side of $\mathcal{S}$ with h positive ($x \in \mathcal{X}_2$). At jumps, if

$g(x) \in \mathcal{X}_1$, then $h(g(x)) < 0$, so z is reset to $h(g(x))$ so that after the jump x is in the flow set; similarly if $g(x) \in \mathcal{X}_2$ at the jump. In this way, solutions flow when $h(x)$ and z have the same sign ($h(x)z \geq 0$) and jump when $h(x)$ evaluated along the solution attempts to take a different sign from that of z ($h(x)z \leq 0$).

B. A numerical simulation model of $\mathcal{H}_{\text{ZCD}}$

Given a hybrid system $\mathcal{H}$ as in (3) and its augmentation with zero-crossing detection $\mathcal{H}_{\text{ZCD}} = (C_{\text{ZCD}}, f_{\text{ZCD}}, D_{\text{ZCD}}, g_{\text{ZCD}})$ in (15), a *hybrid simulator* for $\mathcal{H}_{\text{ZCD}}$ is given by the family of systems $\mathcal{H}^s_{\text{ZCD}}$ parameterized by step size s satisfying $s \in (0, s^*]$, $s^* > 0$. The data of the hybrid simulator $\mathcal{H}^s_{\text{ZCD}}$ is given by $(C^s_{\text{ZCD}}, f^s_{\text{ZCD}}, D^s_{\text{ZCD}}, g^s_{\text{ZCD}})$. The hybrid simulator $\mathcal{H}^s_{\text{ZCD}}$ is given by

$$\begin{aligned} \begin{bmatrix} x_s^+ \\ {z_s}^+ \end{bmatrix} &= \begin{bmatrix} f^s(x_s) \\ 0 \end{bmatrix} =: f^s_{\text{ZCD}} \qquad (x_s, z_s) \in C^s_{\text{ZCD}}, \\ \begin{bmatrix} x_s^+ \\ {z_s}^+ \end{bmatrix} &= \begin{bmatrix} g^s(x_s) \\ h^s(g^s(x_s)) \end{bmatrix} =: g^s_{\text{ZCD}} \quad (x_s, z_s) \in D^s_{\text{ZCD}}, \end{aligned} \tag{18}$$

$$C^s_{\text{ZCD}} := \{(x_s, z_s) \in \mathcal{X} \times \mathbb{R} \ : \ h^s(x_s) z_s \geq 0 \}, \tag{19}$$

$$D^s_{\text{ZCD}} := \{(x_s, z_s) \in \mathcal{X} \times \mathbb{R} \ : \ h^s(x_s) z_s \leq 0 \}. \tag{20}$$

The dynamics of the x component for the flows of $\mathcal{H}_{\text{ZCD}}$ have been replaced by the integration scheme $x_s^+ = f^s(x_s)$, where f^s is constructed from f. The jump map of $\mathcal{H}_{\text{ZCD}}$ has been replaced by g^s_{ZCD} while the flow and jump sets C_{ZCD} and D_{ZCD} have been replaced by the sets C^S_{ZCD} and D^s_{ZCD}, respectively. The function h^s is the discretization of the switching function h. The memory state variable z has been replaced by z_s^+. The operation of z_s is equivalent to that of z in $\mathcal{H}_{\text{ZCD}}$ but discretized. Being that the dynamics of the hybrid simulator $\mathcal{H}^s_{\text{ZCD}}$ are purely discrete, the solutions to $\mathcal{H}^s_{\text{ZCD}}$ are given on discrete versions of hybrid time domains as in [14].

Figure 2 shows a solution to Example 2.1 using the $\mathcal{H}^s_{\text{ZCD}}$ framework and the control modes defined in [2]. Notice that the mode changes are made successfully, and the unicycle reaches the target.

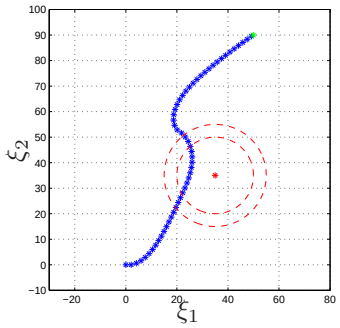

Fig. 2. Solution to Example 2.1 using $\mathcal{H}^s_{\text{ZCD}}$. Solution starts from $(0, 0)$.

IV. Main Results

In this section, we state properties of $\mathcal{H}_{\text{ZCD}}$, results on measurement noise and robustness, and properties of the simulation framework for hybrid systems incorporating zero-crossing detection.

A. Nominal Properties of $\mathcal{H}_{\text{ZCD}}$

Given $\mathcal{H}$ as in (3), we are interested in the conditions on the data of a hybrid system $\mathcal{H}$ under which $\mathcal{H}_{\text{ZCD}}$ has basic regularity properties leading to robustness to perturbations. To that end, the following mild conditions are imposed on the data of $\mathcal{H}$.

Assumption 4.1: Given a hybrid system $\mathcal{H} = (C, f, D, g)$ as in (3) with associated sets $\mathcal{X}$ and $\mathcal{S}$, the following conditions hold:

1) $\mathcal{X}$ is closed (relative to $\mathbb{R}^n$);
2) $f : \mathbb{R}^n \to \mathbb{R}^n$ is continuous on $\mathcal{X}$;
3) $g : \mathbb{R}^n \to \mathbb{R}^n$ is continuous on $\mathcal{X}$;
4) There exists a continuous zero-crossing function h on $\mathcal{X}$ for $\mathcal{S}$.

The following lemma shows that, under these assumptions, $\mathcal{H}_{\text{ZCD}}$ has regular data.

Lemma 4.2: (regularity of data of $\mathcal{H}_{\text{ZCD}}$) Suppose that a hybrid system $\mathcal{H} = (C, f, D, g)$ as in (3) *with associated sets $\mathcal{X}$ and $\mathcal{S}$ satisfy Assumption 4.1. Then, the data of $\mathcal{H}_{\text{ZCD}}$ is such that C_{ZCD} and D_{ZCD} are closed, and f_{ZCD} and g_{ZCD} are continuous.*

When the flows of the hybrid system are transversal to the switching surface and the jump map does not map points back to the jump set, the construction of $\mathcal{H}_{\text{ZCD}}$ is such that it captures all of the solutions to $\mathcal{H}$ (and vice versa).

Proposition 4.3: (properties of solutions to $\mathcal{H}_{\text{ZCD}}$) Given a hybrid system $\mathcal{H} = (C, f, D, g)$ as in (3) *with associated sets $\mathcal{X}$ and $\mathcal{S}$, assume the following:*

1) *$f : \mathbb{R}^n \to \mathbb{R}^n$ is continuous on $\mathcal{X}$;*
2) *There exists a continuously differentiable zero-crossing function h on $\mathcal{X}$ for $\mathcal{S}$ such that*

$$\langle \nabla h(x), f(x) \rangle \neq 0 \qquad \forall x \in D; \tag{21}$$

3) *The jump map g satisfies $g(x) \notin D$ for all $x \in D$.*

Then, for every solution ϕ to $\mathcal{H}$ there exists a solution ψ to $\mathcal{H}_{\text{ZCD}}$ such that $\phi \equiv \psi_x$, where ψ_x denotes the x component of ψ. Furthermore, for every solution ψ to $\mathcal{H}_{\text{ZCD}}$ there exists a solution ϕ to $\mathcal{H}$ such that[1] *$\psi_x \equiv \phi$.*

B. Robustness to measurement noise of $\mathcal{H}_{\text{ZCD}}$

The following result establishes that $\mathcal{H}_{\text{ZCD}}$ is robust to measurement noise. It is proven by embedding the hybrid system $\mathcal{H}_{\text{ZCD}}$ with measurement noise e, denoted $\mathcal{H}^e_{\text{ZCD}}$, into an inflated version of $\mathcal{H}_{\text{ZCD}}$. More precisely, given $\varepsilon_1 > 0$, $\mathcal{H}_{\text{ZCD}}$ is inflated via an outer perturbation giving the perturbed hybrid system

$$\mathcal{H}^{\varepsilon_1}_{\text{ZCD}} : \quad \begin{cases} \dot{x} \in \overline{\text{co}} f_{\text{ZCD}}(x + \varepsilon_1 \mathbb{B}) & x \in C^{\varepsilon_1}_{\text{ZCD}} \\ x^+ \in g_{\text{ZCD}}(x + \varepsilon_1 \mathbb{B}) & x \in D^{\varepsilon_1}_{\text{ZCD}}, \end{cases} \tag{22}$$

[1] There exist solutions ψ' to $\mathcal{H}_{\text{ZCD}}$ that start from D and initially jump due to the value of z, that is, $(0, 1)$ is an element of $\text{dom}\, \psi'$. For such solutions, the equivalence $\psi_x \equiv \phi$ holds for the solution to $\mathcal{H}_{\text{ZCD}}$ defined as $\psi(t, j) = \psi'(t, j + 1)$ for each $(t, j) \in \text{dom}\, \psi'$.

where $\overline{\text{co}}$ denotes the closed convex hull operation,

$$\begin{aligned} C^{\varepsilon_1}_{\text{ZCD}} &:= \{x \in \mathbb{R}^n \ : \ (x + \varepsilon_1 \mathbb{B}) \cap C_{\text{ZCD}} \neq \emptyset \ \} \\ D^{\varepsilon_1}_{\text{ZCD}} &:= \{x \in \mathbb{R}^n \ : \ (x + \varepsilon_1 \mathbb{B}) \cap D_{\text{ZCD}} \neq \emptyset \ \}. \end{aligned}$$

This perturbed hybrid system is such that it captures all of the solutions to $\mathcal{H}^e_{\text{ZCD}}$ with measurement noise $e : \text{dom}\, e \to \varepsilon_1 \mathbb{B}$. Under the conditions in Assumption 4.1, it follows that every solution to $\mathcal{H}^{\varepsilon_1}_{\text{ZCD}}$ is close – in an appropriate sense and on compact hybrid time domains – to an unperturbed solution to $\mathcal{H}_{\text{ZCD}}$. Then, the equivalence result in Proposition 4.3 permits relating these solutions to those of $\mathcal{H}$.

Before presenting the robustness result, we introduce a notion of closeness of hybrid arcs from [13]. The same property can be defined for two discrete arcs as well as for a hybrid arc and a discrete arc; see [14] for more details.

Definition 4.4: ((T, J, μ)-closeness) Given $T, J \geq 0$ and $\mu > 0$, two hybrid arcs $x_1 : \text{dom}\, x_1 \to \mathbb{R}^n$ and $x_2 : \text{dom}\, x_2 \to \mathbb{R}^n$ are (T, J, μ)-*close* if

(a) for all $(t, j) \in \text{dom}\, x_1$ with $t \leq T, j \leq J$ there exists s such that $(s, j) \in \text{dom}\, x_2$, $|t - s| < \mu$, and

$$|x_1(t, j) - x_2(s, j)| < \mu,$$

(b) for all $(t, j) \in \text{dom}\, x_2$ with $t \leq T, j \leq J$ there exists s such that $(s, j) \in \text{dom}\, x_1$, $|t - s| < \mu$, and

$$|x_2(t, j) - x_1(s, j)| < \mu.$$

Theorem 4.5: (robustness of $\mathcal{H}_{\text{ZCD}}$ to measurement noise) Suppose that a hybrid system $\mathcal{H} = (C, f, D, g)$ as in (3) *with associated sets $\mathcal{X}$ and $\mathcal{S}$ satisfy Assumption 4.1 and items 2 and 3 of Proposition 4.3. Let $K \subset \mathbb{R}^n$ be a compact set such that every maximal solution ϕ to $\mathcal{H}$ with $\phi(0, 0) \in K$ is either bounded or complete. Then, for every $\mu > 0$ and every $(T, J) \in \mathbb{R}_{\geq 0} \times \mathbb{N}$ there exists $\varepsilon^* > 0$ such that, for every measurable signal $e : \text{dom}\, e \to \varepsilon \mathbb{B}$, $0 < \varepsilon \leq \varepsilon^*$, every solution ψ^e to $\mathcal{H}^e_{\text{ZCD}}$ with*[2] *$\psi^e_x(0, 0) \in K + \varepsilon \mathbb{B}$, $\psi^e_z(0, 0) = h(\psi^e_x(0, 0))$, is such that there exists a solution ϕ to $\mathcal{H}$ with $\phi(0, 0) \in K$ such that ψ^e_x and ϕ are (T, J, μ) close.*

C. Properties of $\mathcal{H}^s_{\text{ZCD}}$

As pointed out in Section II-B, a hybrid simulator for $\mathcal{H}$ that simply discretizes its dynamics may not be capable of reproducing the jumps of the solutions to $\mathcal{H}$; see, e.g., [11], [12]. As a consequence, solutions to $\mathcal{H}$ cannot be reproduced by $\mathcal{H}^s$ with arbitrary precision. In this section, we present conditions on the data of $\mathcal{H}^s$ that guarantee that when zero-crossing detection is incorporated to it, resulting in the hybrid simulator $\mathcal{H}^s_{\text{ZCD}}$, solutions to $\mathcal{H}$ can be reproduced with arbitrary precision. To this end, the following conditions on the data of $\mathcal{H}^s$ are imposed.

Assumption 4.6: The data f^s and g^s of the hybrid simulator $\mathcal{H}^s = (C^s, f^s, D^s, g^s)$ for the hybrid system $\mathcal{H} = (C, f, D, g)$ and the associated zero-crossing function h^s satisfy the following:

[2] ψ^e_x denotes the x component of ψ while ψ^e_z the z component.

(B0) f^s is such that, for each compact set $K \subset \mathbb{R}^n$, there exists $\rho \in \mathcal{K}_\infty$ and $s^* > 0$ such that for each $x \in C^s \cap K$ and each $s \in (0, s^*]$,

$$f^s(x) \in x + s \ \text{con} f(x + \rho(s)\mathbb{B}) + s\rho(s)\mathbb{B}; \qquad (23)$$

(B1) g^s is such that for any positive sequence $\{s_i\}_{i=1}^\infty$, $s_i \searrow 0$,

$$\lim_{s_i \searrow 0} g^{s_i}(x) = g(x) \qquad \forall x \in \mathbb{R}^n; \qquad (24)$$

(B2) h^s is such that for any positive sequence $\{s_i\}_{i=1}^\infty$, $s_i \searrow 0$,

$$\lim_{s_i \searrow 0} h^{s_i}(x) = h(x) \qquad \forall x \in \mathbb{R}^n. \qquad (25)$$

Integration schemes such as Euler as in Example 2.3 and Runge-Kutta satisfy condition (B0). Conditions (B1) and (B2) hold when the perturbed functions are continuous in the step size; see also [14, Examples 4.8 and 4.9].

When the data of the simulator $\mathcal{H}^s$ and zero-crossing function associated with $\mathcal{H}$ satisfy Assumption 4.6, the data of $\mathcal{H}^s_{\text{ZCD}}$ have regularity properties guaranteeing closeness between the solutions to $\mathcal{H}$ and its simulations obtained via $\mathcal{H}^s_{\text{ZCD}}$. This fact is stated in the next lemma.

Lemma 4.7: (regularity of data of $\mathcal{H}^s_{\text{ZCD}}$) Assume $\mathcal{H}^s = (C^s, f^s, D^s, g^s)$ and h^s are such that Assumption 4.6 hold. Then, $\mathcal{H}^s_{\text{ZCD}} = (C^s_{\text{ZCD}}, f^s_{\text{ZCD}}, D^s_{\text{ZCD}}, g^s_{\text{ZCD}})$ is such that f^s_{ZCD} and g^s_{ZCD} satisfy (B0) and (B1) in Assumption 4.6, and C^s and D^s are such that

(B3) for any positive sequence $\{s_i\}_{i=1}^\infty$ such that $s_i \searrow 0$, $\limsup_{i\to\infty} C^{s_i} \subset C$, $\limsup_{i\to\infty} D^{s_i} \subset D$, where $\limsup_{i\to\infty} C^{s_i}$, $\limsup_{i\to\infty} D^{s_i}$ are the outer limits of the sequence of sets C^{s_i}, D^{s_i}, respectively.

Hybrid simulators $\mathcal{H}^s_{\text{ZCD}}$ with data satisfying (B0)-(B3) are such that, on finite simulation horizons (T, J), their solutions approximate the solutions to $\mathcal{H}$ with arbitrary precision. The following result states this key relationship between the solutions to $\mathcal{H}$ and its simulations via $\mathcal{H}^s_{\text{ZCD}}$. Recall that, as pointed out in Section II-B solutions to $\mathcal{H}$ cannot be reproduced by $\mathcal{H}^s$ with arbitrary precision.

Theorem 4.8: (closeness between solutions to $\mathcal{H}$ and $\mathcal{H}^s_{\text{ZCD}}$) Suppose that a hybrid system $\mathcal{H} = (C, f, D, g)$ as in (3) *with associated sets $\mathcal{X}$ and $\mathcal{S}$ satisfy Assumption 4.1 and items 2 and 3 of Proposition 4.3. Furthermore, suppose $\mathcal{H}^s_{\text{ZCD}}$ satisfies Assumption 4.6. Then, for every compact set $K \subset \mathbb{R}^n$, every $\varepsilon > 0$, and every simulation horizon $(T, J) \in \mathbb{R}_{\geq 0} \times \mathbb{N}$ there exists $s^* > 0$ with the following property: for any $s \in (0, s^*]$ and any solution $\psi^s_x(0, 0) \in K$ there exists a solution ϕ to $\mathcal{H}$ with $\phi(0, 0) \in K$ such that ψ^s_x and ϕ are (T, J, ε)-close.*

Theorem 4.8 is illustrated in the system of Example 2.1 by plotting the solutions for different step sizes. In Figure 3, both the exact solution and simulation solutions are plotted. The closeness between the exact solution (in black) and the simulated solutions (in blue) can be seen. The simulations

solutions converge to the exact solution as the step size is decreased.

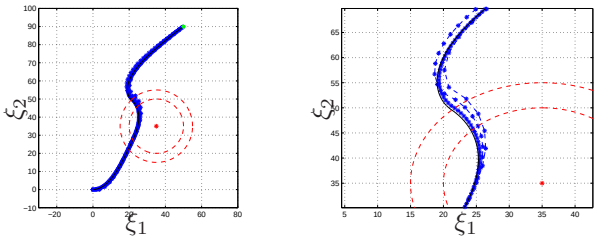

(a) Solution to Example 2.1 with decreasing step size.

(b) Zoomed in solution to Example 2.1 with decreasing step size.

Fig. 3. Closeness between solutions of Example 2.1. Solutions start from $(0, 0)$.

D. Application to hybrid systems $\mathcal{H}$ with asymptotically stable compact sets

In this section, we consider the case when a compact set is asymptotically stable for the hybrid system $\mathcal{H}$ in (3). More precisely, there exists a compact set $\mathcal{A} \subset \mathbb{R}^n$ with the following properties:

- *stable* if for each $\varepsilon > 0$ there exists $\delta > 0$ such that each solution ϕ with $|\phi(0,0)|_{\mathcal{A}} \leq \delta$ satisfies $|\phi(t,j)|_{\mathcal{A}} \leq \varepsilon$ for all $(t,j) \in \operatorname{dom}\phi$;
- *attractive* if there exists $\mu > 0$ such that every solution ϕ with $|\phi(0,0)|_{\mathcal{A}} \leq \mu$ is bounded and if it is complete satisfies $\lim_{(t,j)\in\operatorname{dom}\phi, t+j\to\infty} |\phi(t,j)|_{\mathcal{A}} = 0$;
- *asymptotically stable* if stable and attractive.

Since numerical integration can be interpreted as a perturbation, whether a hybrid simulator will preserve the asymptotic stability properties of $\mathcal{H}$ depends on the effect of perturbations. In light of the lack of robustness of $\mathcal{H}$ to measurement noise pointed out in Proposition 2.2, it is not expected for $\mathcal{H}^s$ to preserve asymptotic stability. However, its version with zero-crossing detection given by $\mathcal{H}^s_{\text{ZCD}}$, when designed with regular data, does preserve stability.

Theorem 4.9: (semiglobal practical stability) Suppose that a hybrid system $\mathcal{H} = (C, f, D, g)$ as in (3) *with associated sets $\mathcal{X}$ and $\mathcal{S}$ satisfy Assumption 4.1 and items 2 and 3 of Proposition 4.3. Furthermore, suppose that $\mathcal{A}$ is a globally pre-asymptotically stable compact set for $\mathcal{H}$ and that $\mathcal{H}^s_{\text{ZCD}}$ satisfies Assumption 4.6. Then, $\mathcal{A}$ is semiglobally practically asymptotically stable for $\mathcal{H}^s_{\text{ZCD}}$, i.e., there exists $\beta \in \mathcal{KL}$ such that, for every compact set $K \subset \mathbb{R}^n$, every $\varepsilon > 0$, and every simulation horizon $(T, J) \in \mathbb{R}_{\geq 0} \times \mathbb{N}$ there exists $s^* > 0$ such that, for each $s \in (0, s^*]$, every solution ϕ^s to $\mathcal{H}^s_{\text{ZCD}}$ with $\phi^s(0,0) \in K$ satisfies for all $(k,j) \in \operatorname{dom}\phi^s$*

$$|\phi^s(k,j)|_{\mathcal{A}} \leq \beta(|\phi^s(0,0)|_{\mathcal{A}}, ks + j) + \varepsilon.$$

The semiglobal practical asymptotic stability property established in the result above holds for sufficiently small step size. The bound s^* on the step size s decreases with ε, which defines the level of closeness to $\mathcal{A}$ that the simulated solutions should arrive at.

Our final result follows from [14, Theorem 5.4] and establishes that the semiglobally asymptotically stable set for $\mathcal{H}^s_{\text{ZCD}}$, denoted $\mathcal{A}_s$, converges to $\mathcal{A}$ as the step size s becomes smaller. In other words, the set $\mathcal{A}_s$ depends continuously on the step size. Below, d_H denotes the Hausdorff distance between two sets.

Theorem 4.10: (continuity of asymptotically stable sets) Suppose the assumptions of Theorem 4.9 hold. Then, there exists $s^* > 0$ such that for each $s \in (0, s^*]$, the hybrid simulator $\mathcal{H}^s_{\text{ZCD}}$ has a semiglobally pre-asymptotically stable compact set $\mathcal{A}_s$ satisfying $d_H(\mathcal{A}_s, \mathcal{A}) \to 0$ as $s \searrow 0$.

V. Conclusion

A mathematical framework for theoretical study of zero-crossing detection algorithms and their effect in simulation of hybrid systems was introduced. Unlike previous work in the literature, the proposed framework allows for analytical study of these properties. The effect of perturbations in hybrid systems jumping on surfaces was highlighted and a hybrid model and simulator incorporating zero-crossing detection were proposed. We establish that when zero-crossing detection is incorporated, the resulting system is robust to measurement noise and to discretization effects in numerical simulation. Our results suggest that integration schemes with zero-crossing detection algorithms actually compute the solutions of a robustified version of the fragile nominal model.

References

[1] D. D. Bainov and P.S. Simeonov. *Systems with Impulse Effect: Stability, Theory, and Applications*. Ellis Horwood Limited, 1989.

[2] M. Boccadoro, Y. Wardi, M. Egerstedt, and E. Verriest. Optimal control of switching surfaces in hybrid dynamical systems. *Discrete Event Dynamic Systems-Theory and Applications*, 15(4):433–448, 2005.

[3] B. Morris and J. W. Grizzle. Hybrid invariant manifolds in systems with impulse effects with application to periodic locomotion in bipedal robots. *IEEE Trans. Aut. Control*, 54(8):1751–1764, 2009.

[4] J. C. Clegg. A nonlinear integrator for servomechanisms. *Transactions A.I.E.E.*, 77(Part II):41–42, 1958.

[5] K. R. Krishnan and I. M. Horowitz. Synthesis of a non-linear feedback system with significant plant-ignorance for prescribed system tolerances. *International Journal of Control*, 19:689–706, 1974.

[6] O. Beker, C.V. Hollot, Y. Chait, and H. Han. Fundamental properties of reset control systems. *Automatica*, 40(6):905–915, 2004.

[7] L. Zaccarian, D. Nesic, and A. R. Teel. First order reset elements and the clegg integrator revisited. *Proc. 24th American Control Conference*, pages 563–568, 2005.

[8] D. D. Bainov and P. S. Simeonov. Systems with impulse effect: Stability, theory, and applications. 1989.

[9] V. Chellaboina, S. P. Bhat, and W. H. Haddad. An invariance principle for nonlinear hybrid and impulsive dynamical systems. *Nonlinear Analysis, Theory, Methods and Applications*, 53:527–550, 2003.

[10] R.G. Sanfelice, R. Goebel, and A.R. Teel. Generalized solutions to hybrid dynamical systems. *ESAIM: Control, Optimisation and Calculus of Variations*, 14(4):699–724, 2008.

[11] J.M. Esposito, V. Kumar, and G.J. Pappas. Accurate event detection for simulating hybrid systems. In *Hybrid Systems: Computation and Control: 4th International Workshop*, pages 204–217, 2001.

[12] F. Zhang, M. Yeddanapudi, and P. J. Mosterman. Zero-crossing location and detection algorithms for hybrid system simulation. In *17th IFAC World Congress*, pages 7967–7972, 2008.

[13] R. Goebel, R. G. Sanfelice, and A. R. Teel. Hybrid dynamical systems. *IEEE Control Systems Magazine*, pages 28–93, 2009.

[14] R. G. Sanfelice and A. R. Teel. Dynamical properties of hybrid systems simulators. *Automatica*, 46(2):239–248, 2010.